Research on Engineering Structures & Materials
www.jresm.org
Research Group

Research Article

Vibrations of nanocomposite beams reinforced by SWCNT sunder the action of harmonic load

Amira Khaldi [a], Sabiha Tekili [b], Youcef Khadri [*,c]

Laboratory for Research in Advanced Technologies in Mechanical Production (LRTAPM), Badji Mokhtar-Annaba University, BP 12, 23000 Annaba, Algeria

Article Info

Article History:

Received 06 July 2025

Accepted 30 Sep 2025

Keywords:

Vibrations;
Beam;
Natural frequency;
Carbon nanotubes;
Nanocomposite;
Harmonic load

Abstract

In this paper, the free and forced vibrations of carbon nanotube-reinforced composite beams are studied using Euler-Bernoulli beam theory. The effective properties of the composite material are estimated using the Mori-Tanaka homogenization technique. Two beam models are considered, the single-walled carbon nanotube (SWCNT) beams with uniformly aligned carbon nanotubes and beams with randomly oriented carbon nanotubes. A MATLAB code is developed to analyze the dynamic response of carbon nanotube-reinforced composite beams subjected to harmonic loading, considering different boundary conditions. The originality of this work lies in the comparative analysis between beams reinforced with aligned and randomly oriented CNTs, under harmonic excitations, which has not been widely addressed in the literature Particular attention is paid to the effect of the carbon nanotube distribution ratio on the natural frequencies and vibration performance. Results indicate that the incorporation of oriented CNTs markedly boosts the stiffness and vibration resistance of the beam. Notably, strategic CNTs alignment leads to higher natural frequencies and reduced displacement.

1. Introduction

Innovative engineering structures require materials capable of supporting both static and dynamic loads. Among these, composite beams have become essential in modern constructions [1]. Studies show that nanocomposite materials, especially those incorporating carbon nanotubes (CNTs), often exhibit remarkably high natural frequencies due to their exceptional structural stiffness [2 and 3]. Moreover, this study addresses buckling and free vibration of porous FGM beams. A parametric survey shows how porosity volume fraction and distribution patterns degrade stiffness and stability margins. Foundation stiffness and grading index can be tuned to regain lost performance. [4]. The natural frequencies of 2D functionally graded Euler–Bernoulli beams with multiple internal cracks resting on a Winkler–Pasternak foundation computed, A finite element technique is built to capture multi-crack locations and stiffness loss. Increasing crack severity and foundation softness lowers the fundamental frequency, while higher FG gradation stiffens the system. [5]. Unlike traditional composites, functionally graded materials (FGMs) adopt a spatial evolution of reinforcements and a gradual transition [6]. The work analyzes the effect of porosity and boundary conditions on the dynamic characteristics of cracked FGM plates. A refined model quantifies changes in frequencies and mode shapes across different edge constraints. Greater porosity and freer boundaries accentuate frequency reductions, while stiffer constraints counteract crack-induced softening. [7]. This structural configuration exhibits lower stiffness than other designs, resulting in greater displacement and higher vibration amplitudes.

[*]Corresponding author: youcef.khadri@univ-annaba.dz
[a]orcid.org/0009-0009-5090-5362; [b]orcid.org/0009-0001-2261-3751; [c]orcid.org/0009-0000-6976-7195
DOI: http://dx.doi.org/10.17515/resm2025-1013ma0706rs

According to reference [8], reducing the volume fraction of carbon nanotubes (CNTs) further amplifies these vibrations. The Mori-Tanaka method was used to estimate the effective material properties of carbon nanotube (CNT)-reinforced composites in [9]. This approach is adaptable to different types of nanocomposites reinforced with straight, aligned, or randomly dispersed carbon nanotubes [10]. Using multi-scale analysis, carbon nanotubes (SWNT) and graded through thickness. Different beam theories (classical, Timoshenko, and parabolic shear deformation) combined with the Rayleigh–Ritz method are applied and validated with finite element simulations. Results show that increasing SWNT content, slenderness ratio, and decreasing power-law index significantly enhance the natural frequencies of the beams, demonstrating the strong reinforcing effect of SWNT [11]. Vodenitcharova and Zhang [12] explored the dynamic behavior of functionally graded double-beam nanocomposite systems infused with single-walled carbon nanotubes (SWCNTs). In [13], the free vibrations of a functionally graded beam were analyzed using the finite element method.

Furthermore, [14] studied CNT-based polymer composites and discovered a powerful effect: the introduction of even a trace of carbon nanotubes can significantly improve the composite's mechanical strength and thermal performance. Piovan and Sampoia [15] analyzed the dynamic response of rotating beams composed of functionally graded materials. Xiang and Yang [16] studied the response of a thermally prestressed, variable-thickness functionally graded laminated beam to free and forced vibrations. Annapoorna K et al. [17] improved the mechanical properties of a new material by using alumina nanoparticles as reinforcements in an aluminum matrix composite. Ke et al. [18] and Virendra Kumar et al. [19] studied the nonlinear free vibration behavior of functionally graded nanocomposite beams embedded with SWCNTs. The impact of CNT volume fraction, distribution patterns, aspect ratio, and dynamic parameters on the forced vibration response of SWCNT beams was extensively examined [20]. Sina et al. [21] presented an advanced beam theory designed to capture the free vibration characteristics of functionally graded beams. A key strategy for vibration control, as discussed in [22], is to adjust the natural frequencies of a structure relative to those of external excitations. Based on this principle, the equations of motion were formulated using the Lagrange method under the Euler-Bernoulli beam assumptions, as demonstrated by Shokrieh and Rafiee [23]. Extending to the nanoscale, [24] performed a nonlinear study of a carbon nanotube embedded in a polymer matrix, using a comprehensive 3D multi-scale finite element model. In this study, we examine the dynamics of composite beams reinforced with carbon nanotubes. Particular attention is paid to the influence of CNT distribution on natural frequencies and overall vibration performance. [25] examines how cracks affect the dynamic response of bidirectional porous FG beams on an elastic foundation via a finite element approach. Material gradation in two directions and uniform porosity is included. Results indicate that crack depth and position strongly decrease frequencies and raise dynamic deflections, with foundation stiffness mitigating the degradation.

2. Material Properties of The Nanocomposite Beams

2.1. Composites Reinforced with Aligned CNT's

Consider a polymer-based composite material incorporating carbon nanotubes. The CNTs were assumed to be non-functionalized and uniformly dispersed, and their effective contribution was calculated through the Mori–Tanaka scheme in MATLAB. the CNTs were assumed to be non-functionalized and uniformly dispersed within the polymer matrix. Functionalization effects, such as improved dispersion or interfacial bonding, were not included the CNTs were assumed to be non-functionalized and uniformly dispersed within the polymer matrix for a unidirectional composite, the CNT modulus is determined in terms of stiffness constants

The effective elastic moduli tensor $\boldsymbol{C}$ is defined analytically as:

$$C = (f_m\, c_m + f_r c_r : A) : (f_m I + f_r A)^{-1} \tag{1}$$

in which f_m , f_r denote volume fractions of the matrix and CNTs (fiber), respectively, while c_m and c_r denote the elastic moduli tensor of the matrix phase and the fiber phase, respectively, $\boldsymbol{I}$ is the

fourth-order identity tensor; then A is : $A = [I + S : (c_m)^{-1} : (c_r - c_m)]^{-1}$, where, S denotes Eshelby tensor. We consider first a polymer composite reinforced with straight CNTs aligned in the x2-axis direction. In case of CNTs' Hill's elastic moduli are not directly available, we can calculate them through CNTs' elastic Young's and shear moduli as well as Poisson's ratio.

$$\begin{bmatrix} n_r & l_r & l_r & 0 \\ l_r & k_r + m_r & k_r + m_r & 0 \\ l_r & k_r - m_r & k_r - m_r & 0 \\ 0 & 0 & 0 & p_r \end{bmatrix} = \begin{bmatrix} \frac{1}{E_{rL}} & -\frac{v_r}{E_{rL}} & -\frac{v_r}{E_{rL}} & 0 \\ -\frac{v_r}{E_{rL}} & \frac{1}{E_{rT}} & -\frac{1}{E_{rT}} & 0 \\ -\frac{v_r}{E_{rL}} & -\frac{1}{E_{rT}} & \frac{1}{E_{rT}} & 0 \\ 0 & 0 & 0 & \frac{1}{G} \end{bmatrix}^{-1} \tag{2}$$

The subscripts L and T represent the longitudinal and normal directions, respectively. The elastic moduli parallel and normal to the CNTs as well as Poisson's ratio are expressed as [10]:

$$E_{11} = n - \frac{l^2}{k}, \quad E_{22} = \frac{4m\,(kn - l^2)}{kn - l^2 - mn}, \quad G_{12} = 2p, \quad v_{12} = \frac{l}{2k} \tag{3}$$

The index*1*and *2* represent the longitudinal and normal directions, respectively. The n, l, k, m, n, represent Hill's elastic moduli, they are given by Mori-Tanaka method:

$$\begin{aligned} k &= \frac{E_m\{E_m c_m + 2k_r(1+v_m)[1 + c_r(1-2v_m)\}}{2(1+v_m)[E_m(1+c_r-2v_m) + 2c_m k_r(1-v_m-2v_m^2)]} \\ l &= \frac{E_m\{c_m v_m[E_m + 2k_r(1+v_m)] + 2c_r k_r(1-v_m^2)\}}{(1+v_m)[2c_m k_r(1-v_m-2v_m^2) + E_m(1+c_r-2v_m)]} \\ \eta &= \frac{E_m^2\ c_m(1+c_r-c_m v_m) + 2c_m c_r(k_r n_r - l_r^2)(1+v_m)^2(1-2v_m)}{(1+v_m)[2c_m k_r(1-v_m-2v_m^2) + E_m(1+c_r-2v_m)} + \\ &\quad \frac{E_m\,[2c_m^2 k_r(1-v_m) + c_r\eta_r(1-2v_m+f_r) - 4c_m l_r v_m}{2c_m k_r(1-v_m-2v_m^2) + E_m(1+c_r-2v_m)} \\ p &= \frac{E_m[E_m c_m + 2p_r(1+c_r)(1+v_m)]}{2(1+v_m)[E_m(1+c_r) + 2c_m p_r(1+v_m)]} \\ m &= \frac{E_m[E_m c_m + 2m_r(1+v_m)(3+c_r-4v_m)]}{2(1+v_m)\{E_m[c_m + 4c_r(1-v_m)] + 2c_m m_r(3-v_m-4v_m^2)\}} \end{aligned} \tag{4}$$

$c_r$andc_m are the volume fractions for carbon nanotube and matrix, $c_m = 1 - c_r$, $E_m$is the matrix Young's modulus, $v_m$is the Poison's ratio and $k_r, l_r, m_r, n_r, p_r$are the elastic modulus for the fiber.

2.2. Composites Reinforced with Randomly Oriented CNT's

This section explores the influence of incorporating straight carbon nanotubes CNTs with completely random orientations into the polymer matrix. Under these conditions, This orientation is characterized by two Euler angles α and β. The base vectors e_i and e_i' of the global $(o - x_1x_2x_3)$ and the local coordinate systems $(o - x_1x_2x_3)$ are related via the transformation matrix **g**

$$\mathrm{e_i} = \mathrm{g_{ij}}\mathrm{e_i'} \tag{5}$$

where g is given by

$$\mathrm{g} = \begin{bmatrix} \cos\beta & -\cos\alpha\sin\beta & \sin\alpha\sin\beta \\ \sin\beta & \cos\alpha\cos\beta & -\sin\alpha\cos\beta \\ 0 & \sin\alpha & \cos\beta \end{bmatrix} \tag{6}$$

The orientation distribution of CNTs in a composite is characterized by a probability density function $p = (\alpha, \beta)$satisfying the normalization condition

$$\int_0^{2\pi}\int_0^{\pi/2} \mathrm{p}(\alpha,\beta)\sin\alpha\,\mathrm{d}\alpha\mathrm{d}\beta = 1 \tag{7}$$

If CNTs are completely randomly oriented, the density function is

$$\mathrm{p}(\alpha,\beta) = \frac{1}{2\pi} \tag{8}$$

According to the Mori–Tanaka method, the strain $\varepsilon_r(\alpha,\beta)$ and the stress $\sigma_r(\alpha,\beta)$ of the CNT are related to the stress of matrix $\sigma_m$by

$$\varepsilon_\mathrm{r}(\alpha,\beta) = \mathrm{A}(\alpha,\beta)\varepsilon_\mathrm{m} = \mathrm{A}(\alpha,\beta)\mathrm{C}_\mathrm{m}^{-1}\sigma_\mathrm{m} \tag{9}$$

the average strain and stress in all randomly oriented CNTs can be written as

$$\langle\varepsilon_r\rangle = \left[\int_0^{2\pi}\int_0^{\pi/2} p(\alpha,\beta)\,A(\alpha,\beta)sin\,\alpha\,d\alpha d\beta\right]\varepsilon_m \tag{10}$$

$$\langle\sigma_\mathrm{r}\rangle = \left[\int_0^{2\pi}\int_0^{\pi/2} \mathrm{p}(\alpha,\beta)[\mathrm{C}_\mathrm{r}\mathrm{A}(\alpha,\beta)\mathrm{C}_\mathrm{m}^{-1}]\sin\alpha\,\mathrm{d}\alpha\mathrm{d}\beta\right]\sigma_\mathrm{m} \tag{11}$$

The angle brackets $\langle\ \rangle$ represent the average over special orientations. Using the average theorems $\sigma = \mathrm{f_m}\sigma_\mathrm{m} + \mathrm{f_r}\langle\sigma_\mathrm{r}\rangle$ and $\varepsilon = \mathrm{f_m}\varepsilon_\mathrm{m} + \mathrm{f_r}\langle\sigma_\mathrm{r}\rangle$ in conjunction with the effective constitutive relation $\sigma = \mathrm{C}\varepsilon$, the effective mechanical proprieties of the nanocomposite are given by

$$E = \frac{9KG}{3K-G}, \qquad \upsilon = \frac{3K-2G}{6K+2G}, \tag{12}$$

For nanocomposite with CNTS randomly oriented the bulk modulus K and shear modulus G are derived as

$$K = K_m + \frac{c_r(\delta_r - 3K_m\alpha_r)}{3(c_m + c_r\delta_r)}, \qquad G = G_m + \frac{c_r(\eta_r - 2G_m\beta_r)}{2(c_m + c_r\beta_r)}, \tag{13}$$

Where;

$$\begin{gathered}
\alpha_r = \frac{3(K_m+G_m)+k_r-l_r}{3(k_r+G_m)},\\
\beta_r = \frac{1}{5}\left\{\frac{4G_m+2k_r+l_r}{3(k_r+G_m)} + \frac{4G_m}{(p_r+G_m)} + \frac{2[G_m(3K_m+G_m)+G_m(3K_m+7G_m)]}{G_m(3K_m+G_m)+m_r(3K_m+7G_m)}\right\}\\
\delta_r = \frac{1}{3}\left[\eta_r + 2l_r + \frac{(2k_r-l_r)(3K_m+2G_m-l_r)}{k_r+G_m}\right],\\
\eta_r = \frac{1}{5}\left[\frac{2(\eta_r-l_r)}{3} + \frac{8G_mp_r}{(p_r+G_m)} + \frac{8G_mm_r(3K_m+4G_m)}{3K_m(m_r+G_m)+G_m(7m_r+G_m)}\right] + \\
\frac{2(k_r-l_r)(2G_m+l_r)}{3(k_r+G_m)}
\end{gathered} \tag{14}$$

In which the bulk modulus K_m and shear modulus G_m of the matrix, which are defined by

$$K_m = \frac{E_m}{3(1-2\upsilon_m)}, \qquad G_m = \frac{E_m}{2(1-\upsilon_m)}, \tag{15}$$

3. Governing Equations

By applying the Euler-Bernoulli beam theory to a beam, the governing equation of motion can be derived. The governing differential equation for forced vibrations of a simply supported beam

$$EI\frac{\partial^4 w(x,t)}{\partial x^4} + \rho A\frac{\partial^2 w(x,t)}{\partial t^2} = F(x,t), \tag{16}$$

The beam considered is a simply supported nanocomposite with a length l, width b, thickness h, Young's modulus, density ρ, transverse deflection w and external load $F(x,t) = F_0 \sin \omega t$ harmonic force as shown in Fig. 1.

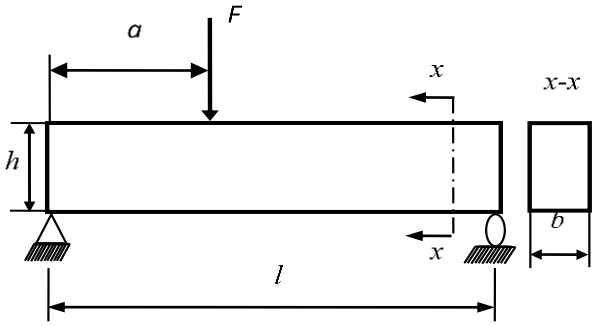

Fig. 1. Geometry of nanocomposite beams reinforced by SWCNTs

The solution of the forced-vibration of a beam can be determined by using the mode superposition principle

$$w(x,t) = \sum_{i=1}^{\infty} \varphi_i(x)\, q_i(t), \tag{17}$$

where $q_i(t)$are generalized modal coordinate,$\varphi_i(x)$ are mode shapes. By multiplying Eq. (9) throughout by$\varphi_i(x)$,integrating from 0 to l, and using the orthogonally condition, we obtain [26]

$$q_i(t) = \frac{\int_0^l \varphi_i(x) w(x,t)dx}{\int_0^l \varphi_i(x)\varphi_i(x)dx} \tag{18}$$

By Substitution eq. (10) in eq. (9) and ,integrating from 0 to l, the result is as flows:

$$EI\, q_i(t)\int_0^l \varphi_i(x)\frac{d^4\varphi_i(x)}{dx^4}dx + \rho A\frac{d^2 q_i(t)}{dt^2}\int_0^l \varphi_i^2(x)dx = F(x,t), \tag{19}$$

The general expression of $\varphi_i(x)$ for the four boundary conditions is given by the following equation

$$\varphi_i(x) = C_1(\cos\beta x + \cosh\beta x) + C_2(\cos\beta x - \cosh\beta x) + C_3(\sin\beta x + \sinh\beta x) + C_4(\sin\beta x - \sinh\beta x) \tag{20}$$

where C_1, C_2, C_3 and $C_4$are constants, which can be found from the boundary conditions Clamped-Clamped (C-C), Clamped-Free (C-F), Clamped-Supported (C-S) and Simply Supported (S-S) as shown in Table 1. For simply supported beam $\varphi_i(x) = sin(i\pi x/l)$, we obtain after integration

$$\frac{d^2 q_i(t)}{dt^2} + \omega_i^2 q_i(t) = \frac{2}{\rho A l}F(x,t) \text{ and } \omega_i = \left(\frac{i\pi}{l}\right)^2\sqrt{\frac{EI}{\rho A}} \quad i = 1,2,\ldots \tag{21}$$

Using the Duhamel integral, the solution of Eq. (13) can be expressed as

$$q_i(t) = \frac{2F_0}{\rho A l}\sum_{i=1}^{\infty}\frac{1}{\omega_i^2-\omega^2}sin\frac{n\pi a}{l}sin\,\omega t \tag{22}$$

Thus, the response of the beam is:

$$w(x,t) = \frac{2F_0}{\rho A l}\sum_{i=1}^{\infty}\frac{1}{\omega_i^2-\omega^2}sin\frac{n\pi a}{l}sin\,\omega t\,sin\frac{n\pi x}{l} \tag{23}$$

Table 1. Different boundary conditions

Beam configuration	C-C	C-F	C-S	S-S
at $x=0$	$w=0, w_x'=0$	$w=0, w_x'=0$	$w=0, w_x'=0$	$w=0, w_x''=0$
at $x=1$	$w=0, w_x'=0$	$w_x''=0, w_x'''=0$	$w=0, w_x''=0$	$w=0, w_x''=0$

4. Results and Discussions

A MATLAB code was developed to solve the governing equations of motion. The algorithm involves a Computing the effective material property of the nanocomposite using the Mori–Tanaka scheme, substituting these properties into the Euler–Bernoulli beam model, applying boundary conditions to obtain eigenvalue solutions for natural frequencies and to determine the dynamic response under harmonic loading. The code was validated by comparing the natural frequencies of isotropic beams with benchmark results from Ref. [11]and [13].

4.1. Engineering Constants of Nanocomposite Beams

Before analyzing the free and forced vibration results of CNT-reinforced composite beams, the engineering constants of these beams were evaluated as a function of Cr. The Young's modulus and Poisson's ratio of polystyrene (matrix) $E_m = 1.9\ (GPa)$ and$v_m = 0.3$, respectively, as well as the Hill elastic moduli of the reinforcement: $k_r = 30$ GPa, $l_r = 10$ GPa, $m_r = 1$ GPa, $n_r = 450$ GPa, $p_r = 1$ GPa, are taken from the Ref. [26]. Figures 2 and 3 show the relationship between the longitudinal Young's moduli with increasing volume fraction of aligned CNT's and randomly oriented CNTs respectively.

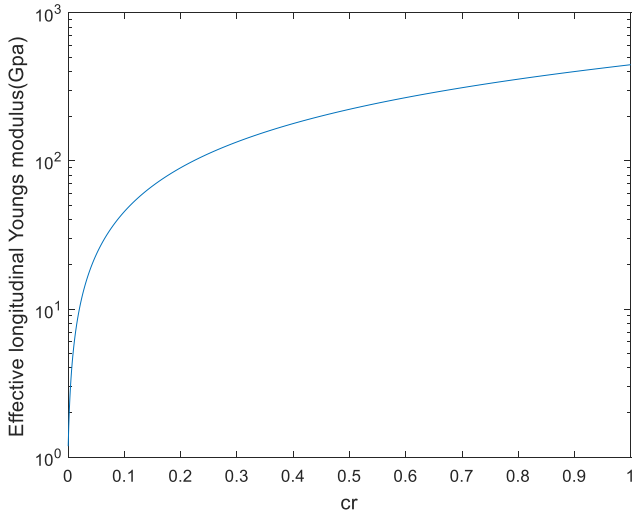

Fig. 2. Young's modulus of aligned

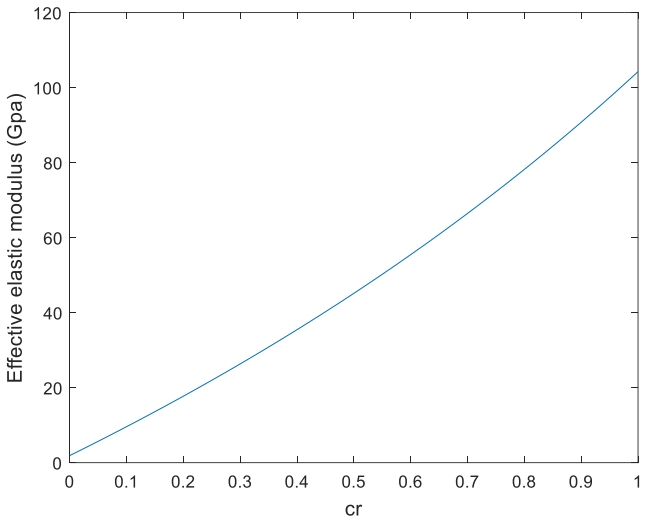

Fig. 3 Young's modulus of randomly oriented

Figure 2 demonstrate a strong dependence of the effective Young's modulus on the volume fraction of CNTs when they are uniformly aligned. A nearly linear or super-linear growth is observed as CNT content increases, highlighting the efficiency of directional reinforcement. The load transfer between matrix and nanotubes is maximized in this configuration, resulting in a substantial improvement in stiffness even at relatively low volume fractions. This behavior confirms that controlled alignment is the most effective strategy for tailoring elastic properties in nanocomposite beams. Figure 3 shows a much weaker enhancement of Young's modulus for randomly oriented CNTs. Although the modulus still increases with CNT fraction, the slope of improvement is significantly lower compared to the aligned case. Random dispersion reduces the reinforcement efficiency because nanotubes contribute equally in all directions, diluting their impact along the beam axis where stiffness is most critical. This isotropic-like effect explains why improvements remain modest and nonlinear, even with higher CNT fractions. The longitudinal Young's modulus of aligned CNT's increases more rapidly with increasing volume fraction of nanotubes than the Young's modulus of randomly oriented CNT's. The maximum improvement in the elastic modulus of carbon nanotube reinforced composites (CNTRCs) is achieved when the carbon nanotubes are uniformly aligned

4.2. Free Vibration

For validation, the present frequencies of isotropic homogeneous beams with material properties (steel) of beam E = 210 GPa and $\rho = 7800\, kg/m^3$, are numerically validated by comparing with available frequencies based on the Euler-Bernoulli beam theory as shown Table 2 to check a written programs for a comparison study is done. The parameters of the beam are width b= 0.4 m, thickness h = 1 m, length L = 20 m. Table 2 compares the first four nondimensional frequencies of simply–simply (S–S) with available results in [13]. As can be seen, the present results agree very well with the results available in Ref. [13].

Table 2. First four frequencies

Present work	Ref. [13]
4.4435	4.3425
8.8855	8.6716
13.3290	12.975
17.7710	17.239

First three frequency parameters of simply supported FG SWNT/Al-alloy beams for (L/h = 5) and 5 % and 10 %SWNT are compared with [11], The material properties E= 84.28 GPA, $\rho = 2631.5\ kg/m^3$ and E= 98.33 GPA, $\rho = 2563\, kg/m^3$,respectively.

Table 3. First two frequencies [11]

SWNT	Present work	Ref. [11]
5 %	3.168251	3.3007
	12.673005	12.614
10 %	3.467590	3.6125
	13.870360	13.8058

For analysis, we used CNTRC beam reinforced with properties available in Ref. [14] the (10,10) the single-walled carbon nanotube (SWCNT) at temperature 300 (K): $\rho_{CNT} = 1400\ Kg/m^3$, longitudinal modulus $E_{11}^{CNT} = 5646.6\ GPa$, transverse modulus $E_{22}^{CNT} = 7080\ GPa$, shear modulus $G_{12}^{CNT} = 1944.5\ GPa$ and Poisson's ratio $\upsilon_{12} = 0.175$ with the volume fraction of the fiber is $c_r = 0.075$. As well as the material properties of the matrix are $\rho_m = 1190\ Kg/m^3$, $E_m = 2.5\ GPa$ and $\upsilon_m = 0.3$, modulus of matrix and Poisson's ratio of matrix, respectively.

Fig. 4 indicate the first mode shapes of CNTRC beams with S–S boundary conditions under different carbon nanotubes (CNT) distribution patterns. The results indicate that variations in CNT distribution have only a minimal impact on the mode shapes. The intensity of curvature varies depending on how the CNTs are aligned. Optimized alignment along the beam axis enhances stiffness, leading to a slightly steeper mode shape with reduced amplitude. In contrast, less effective distributions produce a softer response with greater deflection. This confirms that CNT alignment influences the modal stiffness and frequency without altering the overall shape of the fundamental mode. And an increase in the volume fraction of carbon nanotubes (CNTs) further reduces the beam deflection, which is logical because there is an increase in beam stiffness with increasing carbon fiber content. Fig. 5 shows the first five modes of S-S beam aligned CNTs.

The first four natural frequencies of CNT-reinforced composites are summarized in Table 4 for varying CNT volume fractions and boundary conditions. Across all cases, beams with aligned CNTs consistently exhibit much higher natural frequencies than those with randomly oriented CNTs, highlighting the superior load transfer efficiency of alignment, which maximizes stiffness along the reinforcement direction. In contrast, random orientation reduces effectiveness due to isotropic dispersion. As the CNT volume fraction increases from 0.12 to 0.28, natural frequencies rise steadily, with aligned distributions showing significantly larger gains. This confirms that directional reinforcement strongly amplifies the structural response to added CNT content, whereas in randomly oriented composites, the improvements remain modest and volume fraction alone cannot fully compensate for the lack of alignment. Regarding boundary conditions, the highest frequencies are observed in the clamped–clamped (C–C) case, where beam ends are fully constrained.

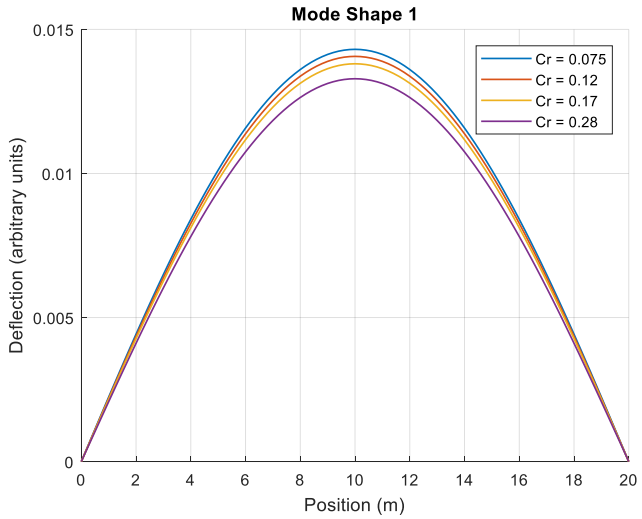

Fig. 4. 1st mode of S-S beam with different distributions of aligned CNTs

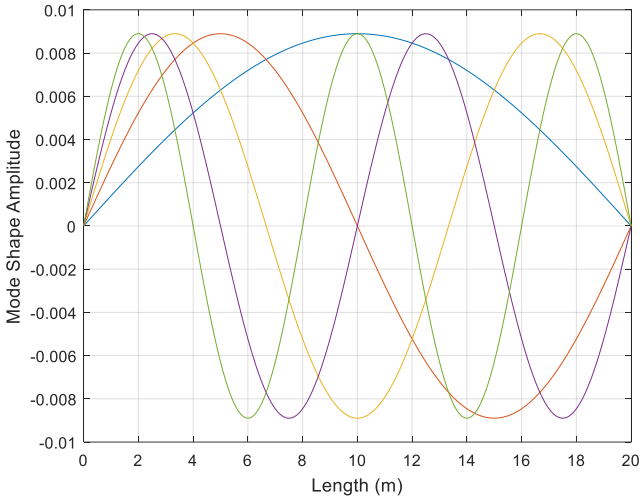

Fig. 5. First five mode of S-S beam aligned CNTs

Intermediate values appear in clamped–simply supported (C–S) and clamped–free (C–F) conditions, while the lowest occur in the simply supported (S–S) case due to its higher flexibility. This frequency hierarchy holds for both aligned and random CNT distributions, though the performance gap is much wider under stiffer constraints. Notably, in the C–C configuration at higher volume fractions, aligned CNTs can produce up to three times the frequencies of random CNT beams, whereas in the S–S case the relative difference diminishes because the flexible supports limit the benefits of alignment.

Table 4. First four frequencies under the Effect of volume fraction

	Aligned CNT's.			Randomly oriented CNT's.		
c_r	0.12	0.17	0.28	0.12	0.17	0.28
C-C	19.0843	20.7602	23.3789	7.9375	8.0034	8.04480
	31.6847	34.4671	38.8149	13.1783	13.2877	13.3564
	44.3659	47.1278	54.3498	18.4526	18.6058	18.7020
	57.0389	62.0479	69.8747	23.7236	23.9206	24.0442
C-F	7.56510	8.2295	9.2675	3.14650	3.1726	3.18900
	18.9390	20.6022	23.2010	7.87710	7.9425	7.98360
	31.6928	34.4759	38.8248	13.1816	13.2911	13.3598
	44.3659	48.2619	54.3498	18.4526	18.6058	18.7020
C-S	15.8444	17.2358	19.4099	6.59000	6.6447	6.67900
	28.5215	31.0261	34.9398	11.8626	11.9611	12.0230
	41.1946	44.8121	50.4648	17.1336	17.2759	17.3652
	53.8717	58.6025	65.9947	22.4062	22.5923	22.7091
S-S	12.6771	13.7904	15.5299	5.27260	5.3164	5.34390
	25.3502	27.5764	31.0549	10.5436	10.6312	10.6861
	38.0273	41.3667	46.5848	15.8163	15.9476	16.0300
	50.7004	55.1527	62.1098	21.0872	21.2624	21.3723

Figs. 6 show the natural frequencies of CNTRC beams with uniformly aligned carbon nanotubes and randomly oriented CNTs in function of volume fraction and boundary conditions different. During design, we aim to maximize the natural frequencies. In our case, the natural frequencies increase with the carbon fiber content of the structure. This is logical because stiffness increases with the fiber content in the beam. For all beams with different boundary conditions, the frequency has the maximum value when c_r=0.28. This effect is more pronounced in the case of uniformly aligned CNTs, where load transfer efficiency is maximized due to directional reinforcement in contrast,

randomly oriented CNTs show a slower and less consistent improvement, reflecting their lower efficiency in enhancing the mechanical properties.

The C-C (clamped–clamped) condition yields the highest natural frequencies due to maximum structural stiffness .and Intermediate values are observed for C-S (clamped–simply supported) and C-F (clamped–free) cases, where partial constraints provide moderate dynamic stiffness. The S-S (simply supported–simply supported) condition produces the lowest natural frequencies, as it represents the least restrictive boundary condition. The difference between aligned and random CNT distributions is most significant under the C-C condition, where the benefits of directional reinforcement are maximized. And for more flexible cases like S-S, the gap between the two distributions diminishes, since the overall structural stiffness is already limited. However, for different boundary conditions, we observe that case (b) Clamped-Free yields maximum frequencies compared to the other cases. Regarding the two configurations of CNTRC beams, used with randomly oriented CNTs and uniformly aligned carbon nanotubes, the latter configuration gives better results, i.e., maximum frequencies compared to the first configuration. This is evident, since the configuration of the beams with fibers aligned in the direction of the beam axis always gives maximum stiffness in the transverse direction of the beam.

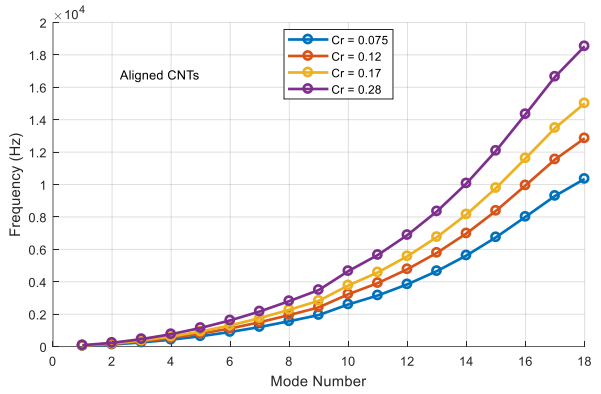

(a) C-C

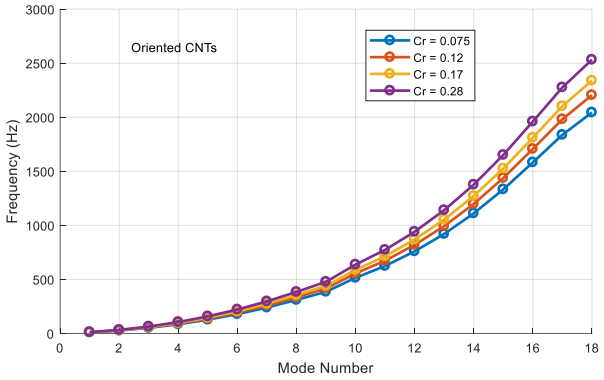

(a) C-C

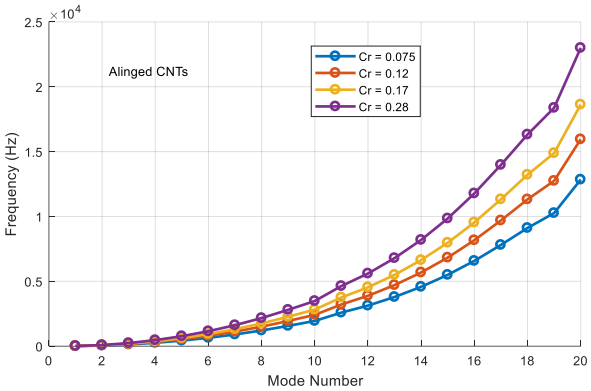

(b) C-F

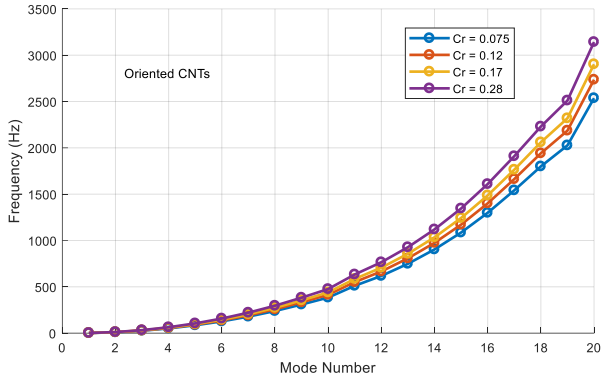

(b) C-F

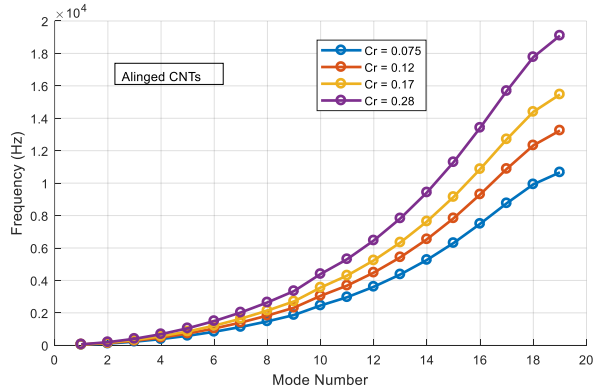

(c) C-S

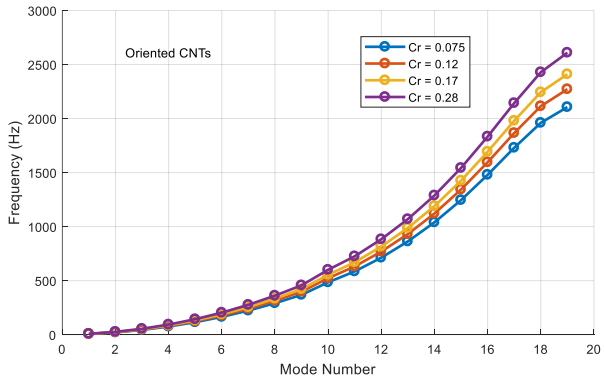

(c) C-S

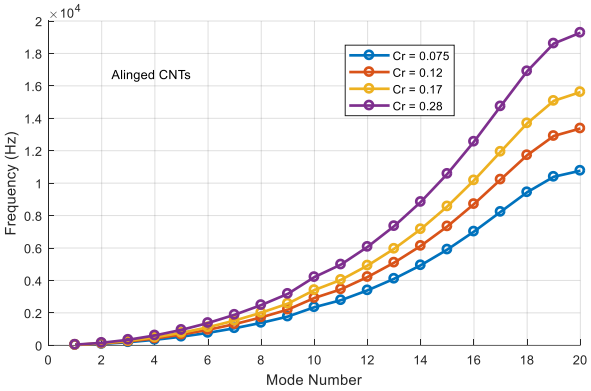

(d) S-S

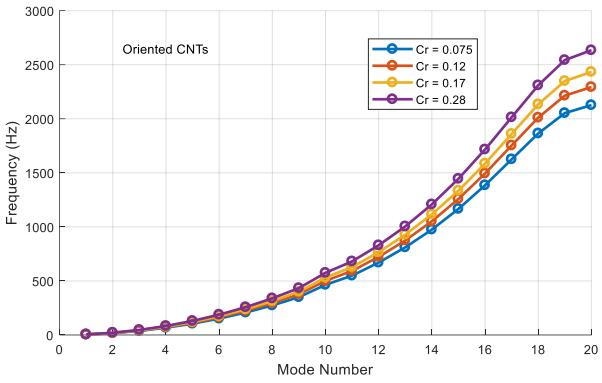

(d) S-S

Fig. 6. Natural frequencies of CNTRC beams with uniformly aligned carbon nanotubes and randomly oriented CNTs in function of volume fraction and boundary conditions different.

4.3. Forced Vibration

In this section, we study the dynamic characteristics of S–S nanocomposite beams under the action of harmonic force $F = F_0 sin \sin \omega t$. The deflection is highest when the force $F_0 = -10\ kN$ and frequency $\omega = 10$ are applied closer to the middle of the beam, particularly at x/L=0.25. Fig. 7 clearly shows that the maximum dynamic response occurs at the position of the applied moving load, which is the mid-span of the beam of the beam (x/L=0.5). Positions closer to the center experience larger deflections, while positions farther away, such as (x/L=0.25 and 0.75), exhibit smaller and nearly similar displacement amplitudes. Although the amplitude varies with position, the oscillation frequency remains identical for all cases, indicating that the moving load excites the same natural frequency regardless of location. This confirms that the dominant response is governed by the first bending mode, which has its maximum displacement at mid-span. Additionally, the similarity of amplitudes at x/L=0.25 and 0.75 reflects the symmetry of the mode shape, reinforcing the fact that boundary conditions and load position strongly control the vibration pattern

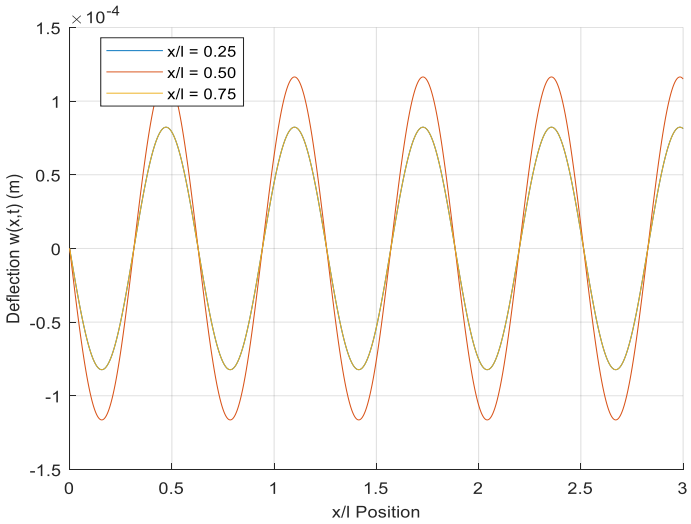

Fig. 7. Transverse displacements of a beam due to x/l position at $c_r = 0.12$

Fig. 8 presents the variation in deflection for beams with different slenderness ratios (L/h=20,40,60,80) at a CNT distribution of c_r =0.12. The results demonstrate that as the slenderness ratio increases, the beam undergoes larger deflections due to reduced stiffness and higher flexibility. This behavior highlights the geometric influence on dynamic response that slender beams are more vibration sensitive, making them more prone to resonance under loads. In contrast, thicker beams (small L/h) resist deflection more effectively, though they may transfer

larger vibration forces to the supports. Moreover, the results suggest that increasing slenderness not only amplifies displacement but also reduces the structural damping efficiency, since vibrations in slender beams decay more slowly. This points to a critical design consideration that slender beams require additional damping or reinforcement to avoid excessive oscillations and resonance problems in dynamic environment.

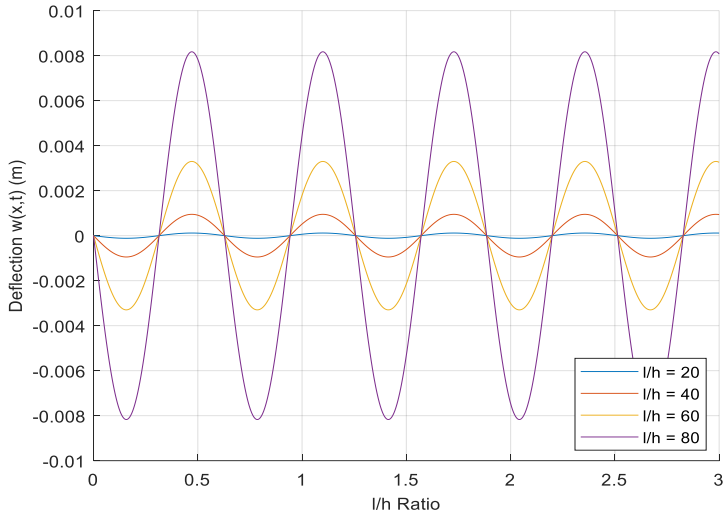

Fig. 8. Effect of beam's slender ratio on the deflection at c_r =0.12

Fig.9 illustrates the variation in the dynamic response of the beam with respect to the load position for different CNT volume fractions. The beam with the lowest fraction (c_r=0.075) shows the largest displacement, while higher fractions lead to a clear reduction in amplitude. This confirms that an increase in CNT content enhances the effective stiffness of the nanocomposite and improves its resistance to dynamic deflection. Moreover, the frequency of oscillation remains nearly unchanged across the cases, indicating that CNT volume fraction mainly affects the amplitude rather than the vibration frequency. An additional observation is that the rate of reduction in deflection becomes less pronounced at higher fractions, which suggests a diminishing reinforcement effect due to matrix–CNT interaction limits. This behavior is important for design, since it shows that beyond a certain volume fraction, additional CNTs may not significantly improve the dynamic responds.

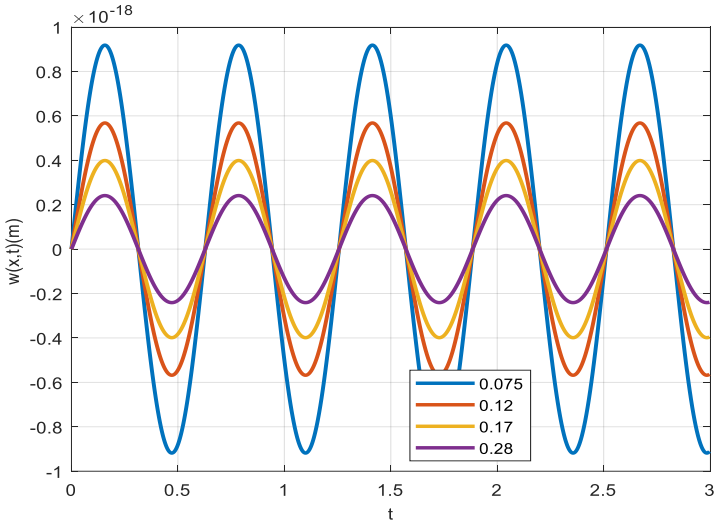

Fig. 9. Transverse displacements of a beam due to x/l position at

Fig. 10 presents a comparison between beams reinforced with aligned and oriented CNTs at a volume fraction of c_r =0.075. The aligned configuration exhibits much smaller deflections than the oriented one, highlighting the strong influence of CNT alignment on stiffness. The superior

performance of aligned CNTs can be attributed to their effective load-transfer mechanism along the beam axis, which is less efficient in the oriented distribution. Furthermore, the aligned case shows a more stable and smoother vibration pattern, whereas the oriented configuration produces higher and more irregular deflections. This implies that manufacturing techniques that control CNT alignment can play a decisive role in optimizing the dynamic performance of nanocomposite beams under moving load.

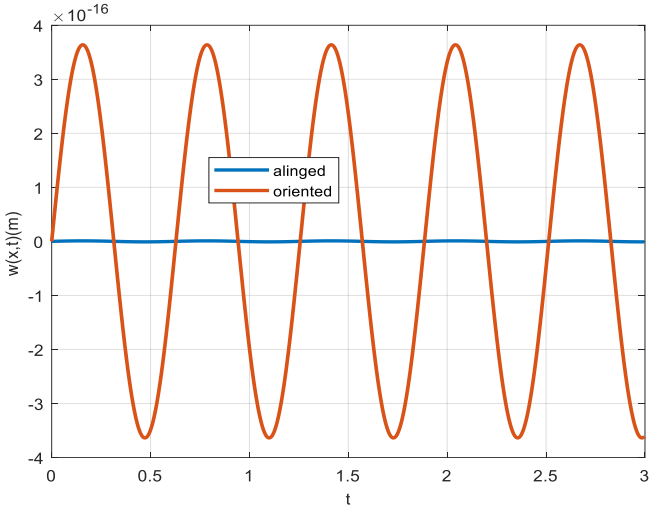

Fig. 10. Effect of beam's slender ratio on the deflection

Fig.11 illustrates the dynamic deflection response of the beam under harmonic excitation at a damping ratio of c_r =0.12. The results show that the peak deflection amplitude increases with the load position, reaching its maximum a=0.75 and a=0.50, while the smallest response is observed a=0.25. This trend indicates that the regions near the mid-span and three-quarter span are more flexible, whereas the quarter span is relatively stiffer. Consequently, the displacement amplitude is strongly influenced by the spatial location along the beam. Overall, the response exhibits a sinusoidal pattern, consistent with the applied harmonic loading, and the amplitude of vibration varies significantly with position along the beam length

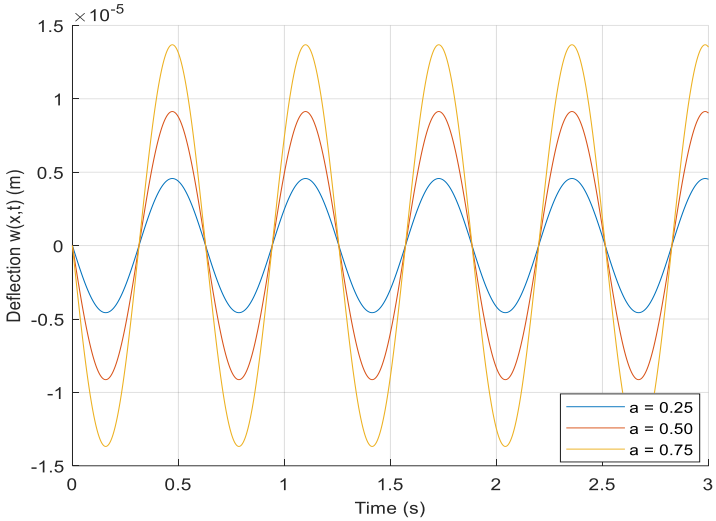

Fig. 11. Transverse displacements of a beam due to x/l position at $c_r = 0.12$

5. Conclusions

This study investigates the free and forced vibration characteristics, along with the dynamic response, of a functionally graded beam. The analysis covers beams reinforced with CNTs, exploring various material distributions, boundary conditions, and CNT arrangements. The findings suggest that enhancing the vibrational performance of CNT-reinforced composites is highly dependent on achieving the CNT's uniform alignment throughout the nanocomposite the dynamic of the beams, particularly their frequencies and deflections. Beams with aligned CNTs, especially the 0.28 distribution, gives the higher natural frequencies and smaller deflections under static harmonic loads, indicating better mechanical performance. Noticing beams with a 0.075 CNT distribution showed the largest deflections, suggesting that CNT distribution plays a crucial role in improving stiffness and reducing deformation. CNT alignment plays a dominant role in vibration performance. Uniformly aligned CNTs yield higher natural frequencies and significantly lower deflections compared with randomly oriented CNTs. In contrast, random CNTs yield only modest improvements, with lower stiffness gains and larger vibration amplitudes, even at higher volume fractions. This improvement is attributed to the efficient load transfer enabled by the high axial stiffness of CNTs Boundary conditions strongly affect the vibrational behavior. Beams with clamped–clamped supports consistently exhibit the highest natural frequencies. with frequency gains up to threefold compared to random distributions, whereas simply supported beams dilute these advantages due to their inherent flexibility. Slenderness ratio influences forced vibration responses that longer beams show larger deflections, whereas shorter beams are more stable. Overall, the findings highlight the importance of CNT distribution in nanocomposite beams for improved vibrational performance, making them promising for advanced structural applications where weight, stiffness, and vibrational characteristics are critical. Future work could extend this investigation to Extend analysis to post buckling and nonlinear vibration regimes, especially under large harmonic excitations or moving loads.

List of Symbols

E_{11}	The elastic moduli parallel for the nanocomposite reinforced by aligned CNTs
E_{22}	The elastic moduli normal for aligned CNTs
ν_{12}	Poisson's ratio
G_{12}	
n, l, k, m, n,	The Hill's elastic moduli
k_r, l_r, m_r, n_r, p_r	The elastic moduli of the fiber
E	The elastic moduli of randomly oriented
c_r	the volume fractions for carbon
c_m	the volume fractions for matrix
E_m	the matrix Young's modulus
ν_m	the Poison's ratio
G	The shear modulus of the nanocomposite
K	the bulk modulus of the nanocomposite
$\alpha_r, \beta_r, \eta_r$	The effective coefficients CNT reinforced composite
K_m	the bulk modulus of the matrix
G_m	The shear modulus of the matrix
$w(x,t)$	transverse deflection
L	The Length of the beam
b	The width of the beam
h	The thickness of the beam
ρ	The density of the beam
$F(x,t)$	The harmonic force
$q_i(t)$	The generalized modal coordinateare
$\varphi_i(x)$	The mode shapes.
ω	The Natural frequency

References

[1] Mohammed, D. and Al-Zaidee, S.R. Deflection reliability analysis for composite steel bridges. Engineering, technology & applied science research, 2022; 12: 9155 – 9159. https://doi.org/10.48084/etasr.5146

[2] Youcef, K., Sabiha, T., El Mostafa, D. et al. Dynamic analysis of train-bridge system and riding comfort of trains with rail irregularities. J Mech. Sci. Technol., 2013; 27:951– 962. https://doi.org/10.1007/s12206-013-0206-8

[3] Zhang, Y.Y., Wang, Y.X., Zhang, X., Shen, H.M. and She, G.L. On snap buckling of FG-CNTR curved nanobeams considering surface effects. Steel Compos. Struct., 2021; 38:293 – 304. https://doi.org/10.12989/scs.2021.38.3.293

[4] Riadh. B, Redhwane . A. A, Fabrice B, Study on stability and free vibration behavior of porous FGM beams, Steel and Composite Structures,2022, https://doi.org/10.12989/scs.2022.45.1.067

[5] Mehdi. G, Samir. Z. Mouloud. D, Natural frequencies of 2D-FG beams with internal crack defects on Winkler–Pasternak elastic foundation using finite element technique, Mechanics Based Design of Structures and Machines ,53,2025.

[6] Zhang, Y.W. and She, G.L. Wave propagation and vibration of FG pipes conveying hot fluid. Steel Compos. Struct.2022: 42: 397-405. https://doi.org/10.12989/scs.2022.42.3.397

[7] Draouche. K, Mohamed .A Amar .M, Lazreg .H, Effect of porosity and boundary conditions on dynamic characteristics of cracked plates made of functionally graded materials, Advances in Concrete Construction.2024, https://doi.org/10.12989/acc.2024.18.3.175

[8] Kiarasi F., Asadi A., Babaei M., Asemi K., Hosseini M., Dynamic analysis of functionally graded carbon nanotube (FGCNT) reinforced composite beam resting on viscoelastic foundation subjected to impulsive loading. Journal of Computational Applied Mechanics, 2022; 53: 1-22. https://doi.org/10.22059/JCAMECH.2022.339008.693

[9] Tsai J-L, Tzeng S-H, Chiu Y-T. Characterizing elastic properties of carbon nanotubes/polyimide nanocomposites using multi-scale simulation. Compos Part B Eng. 2010; 41:106–15. https://doi.org/10.1016/j.compositesb.2009.06.003

[10] Shi D-L, Feng X-Q, Huang YY, Hwang K-C, Gao H. The effect of nanotube waviness and agglomeration on the elastic property of carbon nanotube-reinforced composites. J Eng. Mater Technol., 2004; 126:250–7. https://doi.org/10.1115/1.1751182

[11] Abdellatif Selmi1, Awni Bisharat2, Free vibration of functionally graded SWNT reinforce aluminum alloy beam, Journal of Vibroengineering, ISSN PRINT 1392-8716, ISSN ONLINE 2538-8460, KAUNAS, LITHUANIA, DOI https://doi.org/10.21595/jve.2018.19445

[12] Vodenitcharova T., Zhang L.C., Bending and local buckling of a nanocomposite beam reinforced by a single-walled carbon nanotube, Int. J. Solids Struct., 2006;43:3006–3024. https://doi.org/10.1016/j.ijsolstr.2005.05.014

[13] Amal E. Alshorbagy, M.A. Eltaher, F.F. Mahmoud, Free vibration characteristics of a functionally graded beam by finite element method, Appl. Math. Model. 2011; 35: 412–425. https://doi.org/10.1016/j.apm.2010.07.006

[14] Zhao J., Chen X., et al. Vibration characteristics of functionally graded carbon nanotube reinforced composite double beams in thermal environments, Steel and Composite Structures, 2022; 43:797-808. https://doi.org/10.12989/scs.2022.43.6.797

[15] Piovan M.T., Sampoia R., A study on the dynamics of rotating beams with functionally graded properties, J. Sound Vib., 2009;327: 134–143. https://doi.org/10.1016/j.jsv.2009.06.015

[16] Xiang H.J., Yang J., Free and forced vibration of a laminated FGM Timoshenko beam of variable thickness under heat conduction, Composites: Part B, 2008; 39: 292–303. https://doi.org/10.1016/j.compositesb.2007.01.005

[17] Annapoorna K, Shobha R, et al. Optimization of stir casting parameters for the tensile behavior of nano Al2O3 and ZrO2 reinforced Al-Mg-Si alloy metal composites. Journal of Materials Research and Technology. 2024 August: 10(4), 631–646. http://dx.doi.org/10.17515/resm2024.292ma0518rs

[18] Ke L.L., Yang J., Kitipornchai S., Nonlinear free vibration of functionally graded carbon nanotube-reinforced composite beams, Compos. Struct. 2010; 92: 676–683. https://doi.org/10.1016/j.compstruct.2009.09.024

[19] Virendra Kumar Chaudhari, Achchhe Lal Nonlinear free vibration analysis of elastically supported nanotube reinforced composite beam in thermal environment Procedia Engineering. 2016: 144: 928 – 935. https://doi.org/10.1016/j.proeng.2016.05.119

[20] Civalek Ö., Akba¸s¸ S.D., Akgöz, B. Dastjerdi, S. Forced Vibration Analysis of Composite Beams Reinforced by Carbon Nanotubes. Nanomaterials, 2021; 11:571. https://doi.org/10.3390/nano11030571

[21] Sina S.A., Navazi H.M., Haddadpou H., An analytical method for free vibration analysis of functionally graded beams, Mater. 2009;30: 741–747. https://doi.org/10.1016/j.matdes.2008.05.015

[22] Tilahun ND, Lemu HG. Mechanical vibration analysis of fiber reinforced polymer composite beams using analytical and numerical methods. International Conference on Advances of Science and Technology, 2021; 357-369 http://dx.doi.org/10.1007/978-3-030-80618-7_24

[23] Shokrieh M., Roham Rafiee M., Prediction of mechanical properties of an embedded carbon nanotube in polymer matrix based on developing anequivalent long fiber, Mech. Res. Commun, 2010;37: 235–240. https://doi.org/10.1016/j.mechrescom.2009.12.002

[24] Cheng Z, Zhang N, Gao C, Du X, Zhou S. Amplification factor analysis of a simply supported beam under moving loads. Advances in Mechanical Engineering, 2022; 14(7). https://doi.org/10.1177/16878132221108621

[25] Mouloud .D.Mourad. B,Riadh.B, Effect of crack on the dynamic response of bidirectional porous functionally graded beams on an elastic foundation based on finite element method, Archive of Applied Mechanics, https://doi.org/10.1007/s00419-023-02429-w

[26] Popov, V. N., Van Doren, V. E., & Balkanski, M. J. S. S. C. Elastic properties of crystals of single-walled carbon nanotubes. Solid state communications, 2000; 114(7), 395-399. https://doi.org/10.1103/PhysRevB.61.3078